

TORSION BALANCE TESTS OF SPIN COUPLED FORCES

B. R. HECKEL, for the EotWash Group
Physics Box 351560, University of Washington
Seattle WA 98107, USA
E-mail: heckel@phys.washington.edu

The torque produced on a spin polarized test mass of a torsion pendulum provides a sensitive technique for searching for new weak spin coupled forces. Initial measurements with such a spin polarized torsion balance have provided limits on CPT and Lorentz violating parameters at the level of 10^{-20} eV in the electron sector. A more sensitive version of the spin measurements is in progress.

1 Introduction

The extraordinary sensitivity of the torsion balance instrument has made it a valuable tool to test symmetries in nature and to search for new weak macroscopic forces. Most torsion balance experiments employ unpolarized test bodies either of different composition to test the universality of free fall or of special geometry to test for violations of the inverse square law of gravity.¹ There are several reasons to perform similar torsion balance measurements with a spin polarized test body: to perform a precise test of Lorentz and CPT invariance, to search for new forces mediated by pseudoscalar bosons, and to help elucidate the role of spin in gravitation.

The EotWash group at the University of Washington has constructed an electron spin polarized test body and has completed a first round of measurements with this test body mounted on our EotWash II torsion balance.² In this paper, we present our results and interpret them as a new limit on Lorentz and CPT invariance violation in the electron sector. Improvements to the torsion balance apparatus will be described that should allow us to improve our experimental sensitivity in a second generation experiment that is in progress.

Moody and Wilczek³ have shown that the exchange of a mixed parity boson (such as the axion, a pseudo-scalar particle with a small admixture of scalar coupling) leads to a CP-violating potential between two point particles of the form:

$$V_{1,2}(\vec{r}, \vec{\sigma}_1) = \frac{g_1^P g_2^S}{8\pi m_1 c} \frac{\exp(-r/\lambda)}{r} (\vec{\sigma}_1 \cdot \hat{r}) \left[\frac{1}{\lambda} + \frac{1}{r} \right] \quad (1)$$

where $\vec{\sigma}_1$ and m_1 are the Pauli spin and mass of particle 1, λ is the Compton wavelength of the exchanged boson, and $g^{S(P)}$ is the scalar (pseudoscalar) coupling constant. An interaction of the form of Eq. (1) can be detected as

a non-magnetic torque on a spin in the presence of an unpolarized attractor mass.

Kostelecký and Colladay^{4,5} have developed a general Lorentz invariance-violating extension of the standard model that includes CPT-even and CPT-odd terms. When applied to electrons, the Lorentz-violating lagrangian terms are:⁶

$$L^e = -a_\mu^e \bar{\Psi} \gamma^\mu \Psi - b_{m\nu}^e \bar{\Psi} \gamma_5 \gamma^\mu \Psi - H_{\mu\nu}^e \bar{\Psi} \sigma^{\mu\nu} \Psi / 2 + i c_{\mu\nu}^e \bar{\Psi} \gamma^\mu \vec{D}^\nu \Psi / 2 + i d_{\mu\nu}^e \bar{\Psi} \gamma_5 \gamma^\mu \vec{D}^\nu \Psi / 2 \quad (2)$$

where a_μ^e and b_μ^e are CPT-odd terms and the others CPT-even. For non-relativistic electrons, the lagrangian in Eq. (2) gives rise to a coupling to the electron spin given by:⁶

$$V = \tilde{b}_j^e \sigma_e^j \quad (3)$$

where $\tilde{b}_j^e = b_j^e - m_e d_{j0}^e - \epsilon_{jkl} H_{kl}^e / 2$. The Lorentz and CPT symmetry violation appears as a pseudo-magnetic field, \tilde{b}_j^e , that couples to spin, along an axis fixed in space.

By monitoring the torque on a spin-polarized torsion pendulum as a function of the orientation of the spin relative to both local sources of mass and axes fixed in space, we are able to detect interactions of the forms given by both Eq. (1) and Eq. (3).

2 Spin Polarized Test Mass

To detect anomalous coupling to spin, it is essential to minimize magnetic interactions. Ideally, one would employ a test mass with a non-vanishing spin dipole moment and a vanishing magnetic moment. We approximated this ideal case by constructing an 8-sided ring out of four Alnico magnets and four SmCo magnets, as shown in Figure 1. Eight soft-iron corner pieces allowed the magnet sections to be assembled as an octagon, with the Alnico 5 magnets on one side and the Sm₂Co₁₇ magnets on the other side. After assembly, a coil was wrapped temporarily around the magnet sections and current pulses were sent through the coil to magnetize the Alnico to the same magnetization as the SmCo. The result was a toroidal distribution of magnetization that had essentially the entire magnetic flux enclosed within the octagon.

The net spin polarization comes from the fact that in Alnico, electron spin polarization provides approximately 94% of the magnetization while in Sm₂Co₁₇ electron spin polarization provides only approximately 63% of the magnetization (the remaining fraction comes from the orbital angular momentum of the Sm ions).² Four octagonal rings were stacked with the two center rings rotated by 180° about the net spin axis, giving an A-B-B-A pattern with

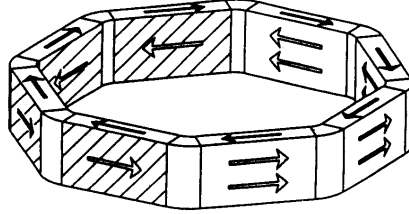


Figure 1: Magnet ring of the spin pendulum. The shaded sections are SmCo magnets and the unshaded are Alnico. The solid arrows on top of the ring show the direction of magnetization. The open arrows on the sides of the ring show the electron spin polarization in each section.

a common spin axis. We estimate that the 64 g of magnets provided a net spin dipole of $(7.8 \pm 0.6) \times 10^{22}$ electron spins that pointed perpendicular to the central axis of the magnet stack.

The remaining components of the spin pendulum were a high permeability cylindrical magnetic shield that surrounded the stack of magnet rings and four right-angle mirrors equally spaced around the midplane of the shield for use by the optical readout system. The dipolar component of the magnetic flux that leaked out of the magnetic shield surrounding the stack of magnets was less than 0.2 mGauss at a distance of 6 cm from the center of the rings, corresponding to a magnetic dipole moment of 0.02 erg/Gauss.

3 Torsion Balance Apparatus

The spin pendulum was mounted within the EotWash II torsion balance apparatus. Because this apparatus is described in detail elsewhere,⁷ only a brief description will be given here. The pendulum was suspended from an 80 cm long, 50 micron diameter tungsten fiber, having a torsion constant of 1.29 erg/rad, and centered within four layers of high permeability magnetic shields. The innermost shield was gold-coated to minimize electrostatic coupling. The pendulum and shields were located within a vacuum vessel that was held to approximately 10^{-6} torr by an ion pump. The vacuum vessel was mounted on a turn-table that rotated at a constant rate of approximately one revolution/hr. A feedback loop locked the output of a precise rotary encoder that

was attached below the rotating vacuum vessel to the frequency of a crystal oscillator to ensure a constant rotation rate.

Other important components of the apparatus included tilt monitors that allowed the rotation axis to be monitored and aligned vertically, constant temperature water-cooled Cu shields that provided thermal isolation, and nearby machined Pb compensator masses that were used to cancel the Y_{21} , Y_{22} , Y_{31} , Y_{41} , and Y_{44} spherical multipole components of the local gravitational field. A set of three-axis Helmholtz coils surrounded the apparatus and were adjusted to cancel the local magnetic field to 1%.

As the vacuum vessel and pendulum within it rotate relative to the laboratory at an angle $\phi = \omega t$, an external potential, V , that couples to spin will produce a torque, $\tau = \partial V / \partial \phi$, causing the spin pendulum to twist by an angle, Θ , relative to the rotating vessel:

$$\Theta(\phi) = V_H \sin(\phi_0 - \phi) / \kappa \quad (4)$$

where κ is the torsion constant of the fiber, V_H is the horizontal component of the coupling to spin, and ϕ_0 is the angle in the horizontal plane at which the coupling is largest. Collimated diode laser light was reflected from one of the four mirrors mounted on the pendulum and the reflected beam was focused onto a linear position sensitive photodiode to monitor the angular position of the pendulum, Θ . A rotary stage at the top of the torsion fiber allowed the light to be centered onto any one of the four symmetrically placed mirrors. As different mirrors were used, ϕ_0 in Eq. (4) was altered by 90° , 180° , or 270° . By adjusting the speed of the turntable at the appropriate times, it was possible to damp the free torsion oscillation of the pendulum, leaving the pendulum essentially at rest in the rotating frame. A magnetic damper plate near the top of the fiber damped most of the other fiber modes.

4 Signal Extraction

The free torsional period, T_0 , of the spin pendulum was 213 s. The rotation period of the turntable was chosen to be either $14T_0$ or $20T_0$. At each rotation rate, data was taken on all four mirrors of the pendulum, comprising eight data sets. We divided the raw data into 'cuts' that consisted of three complete revolutions of the turntable. Each cut was then filtered to remove the free torsional oscillation (by averaging the data over 213 s) and fit to a Fourier series out to the fourth harmonic of the turntable frequency in addition to an offset and linear drift term.⁷ An external coupling to spin will appear in the first harmonic of the Fourier series. The higher harmonics (due to imperfections in the turntable rotation rate and gravity gradient couplings) were monitored for

stability. The cuts from each data run were then averaged and the scatter of the results provided an estimate of the error.

Only two corrections were made to the results. The first was an attenuation correction that accounted for the effects of the pendulum inertia, electronic time constants, and signal averaging on the amplitudes and phases of the harmonic signals.⁷ The second correction was for tilt: if the rotation axis was not exactly vertical, the bending of the fiber at its upper attachment point lead to a fiber twist that varied as the first harmonic of the turntable rotation frequency. Because the tilt of the floor changes by several μrad each day, it was necessary to remove the tilt feed-through from our signal. We did so by deliberately tilting the apparatus in orthogonal directions to calibrate the fiber's sensitivity to tilt. The readings of the tilt monitors for each cut were then used with the measured tilt sensitivity to derive a correction.⁷

Between data sets, additional measurements were made to examine sources for systematic errors: temperature effects, magnetic coupling to the pendulum, and gravitational gradients. In each case, the driving term was greatly exaggerated. The temperature of the apparatus, normally constant to 0.1 mK, was made to vary by 1 K at the turntable rotation frequency. The current in the Helmholtz coils was reversed, increasing the static magnetic field at the apparatus by a factor of 200. The machined Pb gravity gradient compensators were rotated to add to the local gradients rather than cancel them, increasing the gradients by a factor of typically 100. Surprisingly, the magnetic coupling with the Helmholtz coils reversed was almost undetectable, leading to a systematic error of only 0.03 nrad. Gravity gradients and temperature effects were larger sources for systematic error, both at the level of 0.5 nrad.

The largest systematic error was associated with tilt. Although we could reliably correct for slowly varying tilts of the rotation axis, the turntable bearing introduced a reproducible wobble of the rotation axis. Because we could not exaggerate the size of the wobble, we were unable to measure its contribution to the first harmonic component of Θ . Our measured sensitivity to tilt times the magnitude of the wobble leads to a systematic error of 4 nrad.

5 Results for Lorentz Symmetry Violation

To search for a pseudo-magnetic field that violates Lorentz and possibly CPT invariance, as described in Eq. (3), we follow the convention of Bluhm and Kostelecký⁶ to define the nonrotating coordinate axes of \tilde{b}_j^e . The \hat{z} axis is taken to lie along the rotational north pole of the earth: a coupling of the spin pendulum to \tilde{b}_z^e will produce a signal that does not vary as the earth rotates. The \hat{x} axis points from the earth towards the sun at the vernal equinox. Both

Table 1: Spin pendulum results for Lorentz symmetry violation

Data Set	Period	Mirror	$\tilde{b}_x^e (10^{-20} eV)$	$\tilde{b}_y^e (10^{-20} eV)$	$\tilde{b}_z^e (10^{-20} eV)$
1	$14T_0$	1	-6.7 ± 6.5	5.5 ± 6.5	-6.1 ± 8.9
2	$14T_0$	2	4.0 ± 6.2	1.7 ± 6.2	-15.3 ± 7.1
3	$14T_0$	3	4.1 ± 7.6	0.4 ± 7.6	-20.5 ± 9.4
4	$14T_0$	4	3.8 ± 5.3	-2.2 ± 5.3	8.4 ± 7.4
5	$20T_0$	1	-0.2 ± 5.4	-0.4 ± 5.4	1.3 ± 7.8
6	$20T_0$	2	-9.5 ± 6.4	14.5 ± 6.4	-18.4 ± 9.6
7	$20T_0$	3	-0.3 ± 5.2	-5.5 ± 5.2	-16.3 ± 6.8
8	$20T_0$	4	5.7 ± 6.0	-0.7 ± 6.0	-15.4 ± 8.8
Averaged Results			0.1 ± 2.1	1.7 ± 2.3	-10.3 ± 3.9
Systematic Error			± 0.8	± 0.8	± 7.1

the amplitude, V_H , and phase, ϕ_0 , of the spin coupling in Eq. (4) will vary as the laboratory coordinates rotate relative to the \tilde{b}_x^e and \tilde{b}_y^e celestial axes.

For each cut within a data set, we compute the angular coordinates of our spin pendulum relative to the celestial axes. We then fit all of the first harmonic signals from the cuts to a function that describes the amplitude and phase of a coupling to any of the celestial axes.⁸ The results of the fits for each of the eight data sets are shown in Table 1.

The systematic errors for \tilde{b}_x^e and \tilde{b}_y^e in Table 1 are smaller than that for \tilde{b}_z^e because only the components of temperature, magnetic field, gravity gradients, and turntable wobble that vary over the course of a sidereal day contribute to \tilde{b}_x^e and \tilde{b}_y^e , while their average values contribute to \tilde{b}_z^e .

We therefore find no evidence for Lorentz or CPT symmetry violation and quote our results as:

$$\begin{aligned}
 \tilde{b}_x^e &= (0.1 \pm 2.1 \pm 0.8) \times 10^{-20} eV \\
 \tilde{b}_y^e &= (1.7 \pm 2.3 \pm 0.8) \times 10^{-20} eV \\
 \tilde{b}_z^e &= -(10.3 \pm 3.9 \pm 7.6) \times 10^{-20} eV
 \end{aligned}
 \tag{5}$$

where the first error is statistical and the second systematic. Upper limits derived from Eq. (5) provide the most sensitive test, to date, for Lorentz symmetry violation in the electron sector.

6 Second Generation Experiment

To improve upon the results presented in the previous sections, we are in the process of modifying the experimental apparatus in anticipation of a second round of measurements. The statistical error on our measurements should decrease by a factor of 30 due to two factors. The first is from the use of a thinner torsional fiber to reduce the torsion constant of the fiber by a factor of 16. To do so, the mass of the pendulum must be reduced. Most of the mass of the original pendulum came from the magnetic shield that surrounded the stack of magnet rings. We have developed a better way to match the magnetizations of the Alnico and SmCo magnets in the rings and have eliminated the need for a magnetic shield to surround the magnets. With the unshielded stack of magnets, we can halve the thickness of the torsional fiber, giving us 16 times larger angular displacements for the same spin coupling as before. The second factor of improved sensitivity comes from replacing the stepper motor that drove the turn-table by a synchronous motor that allows higher rotation rates (reduced $1/f$ noise) and better rotation speed control. Data taken with the new motor has a signal to noise ratio a factor of two higher than with the stepper motor.

Increased statistical precision is only useful if the systematic errors can be reduced by a comparable factor. The dominant systematic error came from drifts of the tilt angle of the rotation axis. We have installed new leveling feet on the apparatus that are fed-back to the inclinometers that monitor the rotation axis. The feet are made from annuli of Pb that sandwich a plate of Cu. On the Cu plate is a Peltier element that heats or cools the Pb so that the thermal expansion of the Pb can counteract the μrad changes of tilt of the floor. With the thermal feedback system in operation, the rotation axis stays aligned with vertical to 10 nrad, representing a factor of improvement of 300.

We anticipate a factor of 30 increase in experimental sensitivity with the modified apparatus for the spin-coupled signals that have a diurnal variation. For the lab fixed signal (due to \tilde{b}_z^e), we will have to experimentally determine at what level magnetic and gravity gradient systematic errors appear.

Acknowledgments

The team that contributed to the results presented here and to the modifications of the apparatus are: E.G. Adelberger, S. Baessler, J.H. Gundlach, M.G. Harris, U. Schmidt, H.E. Swanson, and M. White. We gratefully acknowledge the financial support for this work provided by the NSF (Grants PHY-9602494 and PHY-9970987) and the DOE through its support of the Center for Nuclear Physics and Astrophysics (Grant DE-FG03-97ER41020).

References

1. E.G. Adelberger, B.R. Heckel, C.W. Stubbs, and W.F. Rogers, *Annu. Rev. Nucl. Part. Sci.* **41**, 269 (1991).
2. M.G. Harris, Ph.D. thesis, Univ. of Washington, unpublished (1998).
3. J.E. Moody and F. Wilczek, *Phys. Rev. D* **30**, 130 (1984).
4. D. Colladay and V.A. Kostelecký, *Phys. Rev. D* **55**, 6760 (1997).
5. D. Colladay and V.A. Kostelecký, *Phys. Rev. D* **58**, 1 (1998).
6. R. Bluhm and V.A. Kostelecký, *Phys. Rev. Lett.* **84**, 1381 (2000).
7. Y. Su, B.R. Heckel, E.G. Adelberger, J.H. Gundlach, M. Harris, G.L. Smith, and H.E. Swanson, *Phys. Rev. D* **50**, 3614 (1994).
8. S. Baeßler, B.R. Heckel, E.G. Adelberger, J.H. Gundlach, U. Schmidt, and H.E. Swanson, *Phys. Rev. Lett.* **83**, 3885 (1999).